Eur. Phys. J. D **43**, 105–108 (2007)
DOI: 10.1140/epjd/e2007-00068-x

THE EUROPEAN PHYSICAL JOURNAL D

Solvation of K^+ in helium droplets

E. Yurtsever[1,a], E. Yildirim[2], M. Yurtsever[2], E. Bodo[3], and F.A. Gianturco[3]

[1] Chem. Dep., Koç Uni. Istanbul, Istanbul 34450, Turkey
[2] Chem. Dep., Istanbul Tech. Uni., Istanbul 34469, Turkey
[3] Chem. Dep., University of Rome "La Sapienza", Rome 00185, Italy

Received 24 July 2006 / Received in final form 19 September 2006
Published online 24 May 2007 –

Abstract. Solvation of K^+ in helium droplets is studied by classical simulation methods. We have previously shown that additive potentials can be used to describe structures of helium droplets when an ionic species is present. Here, we present an accurate ab-initio potential for the K^+ – He interaction. Global minima of KHe_n^+ for up to $n = 70$ are searched for employing Basin Hopping Monte Carlo simulations with a random growth scheme. The extent of the solvation is analyzed. A clear formation of two shells with 15 and 23 atoms is detected.

PACS. 34.20.Cf Interatomic potentials and forces – 36.20.Ey Configuration (statistics and dynamics)

1 Introduction

Helium droplets are known to be the ultimate matrix for the experiments at extremely low temperatures. These ultracold homogeneous matrices are of great importance since they facilitate the synthesis of new molecular complexes [1]. They also serve as suitable containers for neutral or charged atoms and molecules [2] and their absorption and emission spectra can be studied by laser-induced fluorescence techniques [3]. In the recent years, the study of ion containing helium droplets has become more important since they offer an opportunity to probe different aspects of superfluidity [4], the microscopic interactions between the charged impurity and the matrix and to perform experiments for testing the accuracy of the microscopic theories. They are also known to undergo "electrostriction" within the cluster and to give rise to regular patterns of solvent localization around the doping ion known as "snowballs".

The M^+-Rg complexes (M = alkali metal, Rg = rare gas atom) have been studied by various experimental techniques [5]. They are of great interest as the fragmentation products formed upon ionization of the droplets by electron impact just after immersing the impurity. The end products are usually clusters containing the cation with a few helium atoms attached to it. Even though these systems are composed of closed-shell singly charged cations interacting with a bath of closed-shell atoms, there are some interesting structural and dynamical questions as to the possible formation of clear shell structures [4]. The charge delocalization is very small so these clusters can be understood in terms of the solvation of a cationic, well localized region.

[a] e-mail: eyurtsev@ku.edu.tr

Various interaction potentials for M^+-Rg systems have been obtained by experimental and theoretical means. These functions usually consist of two components: (a) a short range repulsive potential and (b) a long range attractive potential. The second term dominates the interaction and can be described in terms of a charge(cation)-induced multipole interaction.

Such characteristics of the interactions of $M(Rg)_n^+$ species allow us to pursue the possibility of using additive potentials to elucidate the solvation of charged impurities in helium droplets. Previously, we have shown that additive potentials provide qualitatively correct information on the structures of small $LiHe_n^+$ clusters [6,7]. The similarities between structures obtained from fully quantum mechanical calculations and those obtained from classical optimization techniques further allow us to use classical simulation techniques to obtain structural information of larger clusters.

In this study, we computed an accurate interaction potential for K^+–He complex and utilized this potential function to study the solvation shells in KHe_n^+. Optimizations are carried out by a modified Basin hopping Monte Carlo algorithm. A scheme is also developed to model the growth of a cluster.

2 An outline of computational tools

2.1 K^+–He interaction

The interaction potential energy curve for the diatomic complex K^+He is calculated by the Coupled-Cluster Singles Doubles including triple excitations non-iteratively CCSD(T) with an aug-cc-pv5z quality basis set. This basis

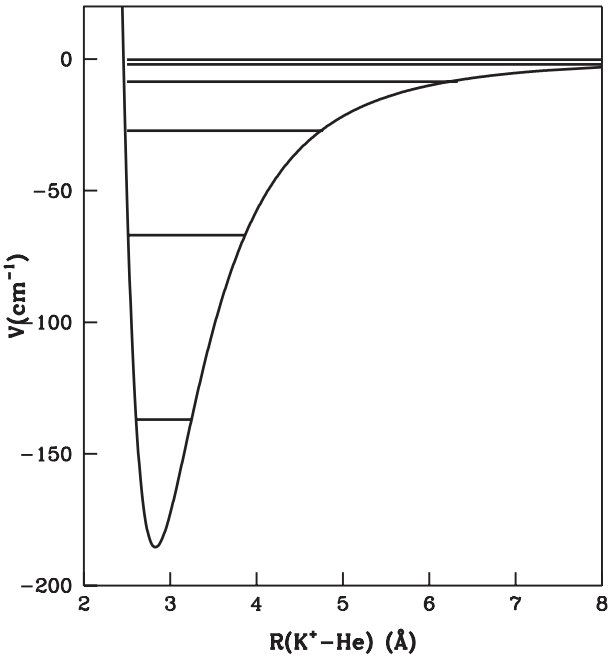

Fig. 1. Potential curve for the K^+–He interaction.

was generated [8] by the augmentation with a large flexible valence basis sets and contraction of the effective core potential (ECP10MWB) [9]. The calculations were carried out with the MOLPRO software [10]. Basis set superposition errors are corrected with the counterpoise method. The resulting potential is given in Figure 1.

The well depth and equilibrium internuclear separation were found to be 185.5 cm^{-1} and 2.83 Å. The potential well supports 6 bound vibrational levels. The results are in very good agreement with empirical potentials [11] as well as calculated ones [12]. This potential has been then fitted to an analytical form:

$$V(r) = e^{-\beta(r-r_0)} \sum_{k=0}^{n-1} a_k (r - r_0)^k - a_n \frac{f_4(\beta r)}{r^4} \quad (1)$$

where $f_n(\beta r)$ is a damping factor of the form:

$$f_n(\beta r) = 1 - e^{-\beta r} \sum_{k=1}^{n} \frac{r^k}{k!} \quad (2)$$

where $\beta = 4.09936$ $Å^{-1}$ and $r_0 = 2.3$ Å. The summation in equation (1) has 17 parameters and they are given in Table 1. The last parameter a_n has been chosen in order to yield at large distances the correct charge-He polarization potential $-\alpha(\mathrm{He})/2r^4$ with $\alpha(\mathrm{He}) = 1.38$ a.u.

For He–He interaction, we have used the Tang-Toennies [13] potential and the sum-of-potentials model has been employed to generate the overall potential among partners within each cluster of size N (the number of solvent atoms).

Table 1. Parameters for K^+–H interaction.

k	a_k
1	765.807
2	–923.112
3	–250.866
4	–5031.64
5	21402.7
6	–64537.6
7	129784
8	–182002
9	180048
10	–126624
11	63184.1
12	–22108.9
13	5282.50
14	–818.502
15	73.977
16	–2.961818
17	11875.0

2.2 Classical optimization

Basin hopping Monte Carlo (BMHC) is a global optimization algorithm which combines a conjugate gradient optimization with a large-step Monte Carlo simulation [14,15]. For large and especially weakly bound clusters, to find the global minimum is very difficult because of the exponentially large number of local minima. These minima may also be separated by large barriers along the phase space. In order to overcome these barriers, large amplitude moves are introduced and these trial moves are accepted or rejected with Boltzmann probabilities as in the importance sampling MC. After such moves, a conjugate gradient optimization is applied to locate a minimum and form a data base of local minima. This method has two adjustable control parameters as the temperature and the amplitude of atomic displacements.

For complex potential-energy-surfaces (PES), finding the global minimum from a single trajectory is a difficult task even for sophisticated methods such as genetic algorithms or BHMC. In particular, escaping from a funnel in the PES may require either a systematic formation of a database of minima or running multiple trajectories to achieve a nearly complete span of the phase space. For the problem of KHe_n^+, there is an additional complication given by the fact that, even though He–He interaction is very weak compared to that of K^+–He, it still dominates the interactions when the helium atom is far away from the ion. Consequently, optimization algorithms may spend a great deal of time trying to optimize He–He interactions. In this work we have devised a growth scheme to overcome this problem. Each new cluster is generated by randomly placing a helium atom in the vicinity of the cluster. Distance of this atom is taken as the radius of the outermost shell and the angular coordinates are chosen randomly. Minima located from these structures are added to a database. After running a sufficient number of trajectories, the lowest energy structure is used to generate the next one. We have used a simple convergence

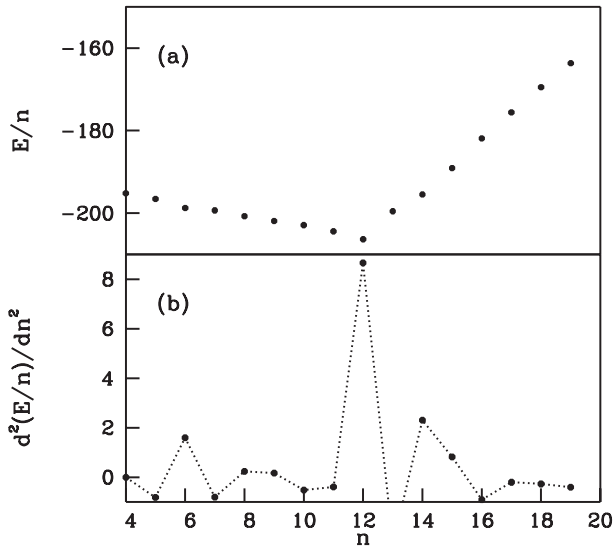

Fig. 2. (a) Variation of energy and (b) its second derivative with size. E is in cm^{-1}.

criterion where it is assumed that the global minimum is found if three new sequences do not produce lower energy structures. In this report, 100 such sequences are generated up to He_{70}.

3 Results

In Figure 2, we present E/n and $d^2(E/n)/dn^2$ for up to $n = 20$. Here E denotes the total interaction energy obtained by additive potentials. The second derivative of the energy calculated from the central difference formula can be used to identify magic numbers as it compares the energy of three successive sizes.

One of the interesting aspects of clusters is the strong size-dependent nature of their physical properties. For example, the stability of the global minima may display an irregular behavior with increasing size. The case of Lennard-Jones clusters is well documented [16] with a number of magic sizes. Here, we present various aspects of the lowest energy structures of KHe_n^+ clusters to understand the growth process and the solvation. It is important to note that, the global minima could be elusive to optimization techniques even for stable systems. The structures presented here are obtained from exhaustive searches over the PES and they should be treated as close approximations to the global minima.

In Figure 2a, it is seen that the energy per particle decreases until $n = 12$ and at this size $d^2(E/n)/dn^2$ has a maximum showing strong stability, almost a magic number behavior. For $n > 12$, average energy increases monotonically. Even though Figure 2 gives the impression that the first solvation shell is completed at 12 atoms, a careful study of structures shows that the growth of KHe_n^+ clusters display several features. When a few helium atoms are present, they form a cluster where the cation rests at its surface. The largest of these clusters is for $n = 8$ and its structure is given in Figure 3.

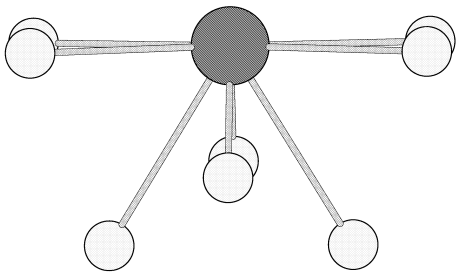

Fig. 3. The lowest energy structure for KHe_8^+.

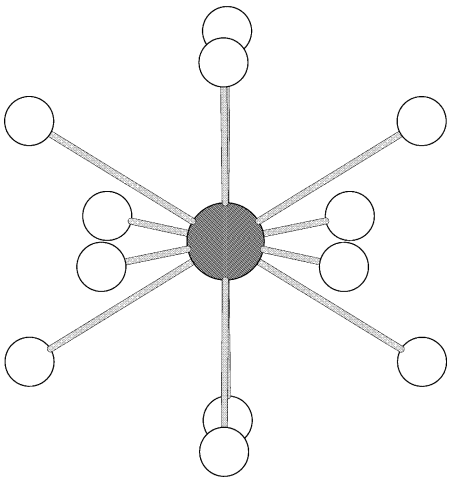

Fig. 4. The lowest energy structure for KHe_{12}^+.

All clusters with less than 8 helium atoms have the same characteristics of this hemispherical structure. At this size range, helium atoms can still orient themselves in such a manner that they are both close to the cation and at the same time they can maximize the number of He–He contacts. At $n = 9$, the solvation starts and the new atoms cause K^+ to drift into the droplet. The internuclear distances between helium atoms and K^+ remain around 2.2–3.1 Å. That is, the new atoms are still added to the first solvation shell. At $n = 12$, a completely symmetric shell is formed where all the K^+–He distances are equal at 2.825 Å. The fact that this bond length is very close to the He–He equilibrium distance allows the formation of a spherical and highly stable structure. The three axes of inertia are all equal to each other. This symmetric top structure is only observed at $n = 12$ (Fig. 4) and forms the basis of its stability.

For $n = 13$–15, new atoms are again added to the first solvation shell. Helium atoms are no longer occupying equivalent positions and the shell radius increases slightly. Only at $n = 16$, an odd atom resides outside the first solvation shell.

We proceeded to search for the lowest energy structures with our growth model until $n = 70$. The results can be summarized in the following manner. From analysis of interatomic distances, we see that the second solvation shell starts to form around $r = 4.2$ Å. At this range the K^+–He potential is still strong enough (47 cm^{-1} compared to 8 cm^{-1} for He–He) so a shell structure can be formed.

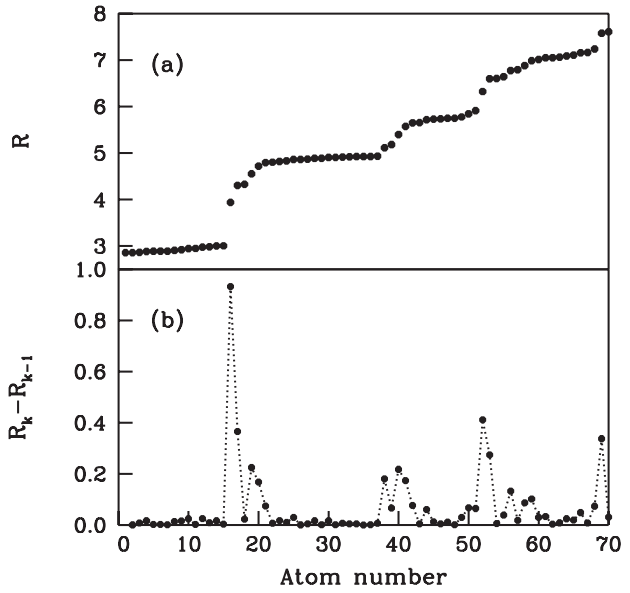

Fig. 5. (a) The variation of $R(K^+–He)$ in KHe_{70}^+ and (b) its derivative. Distances are in Å.

However, both the energy and its derivatives with respect to the size are smoothly varying functions and do not reveal any information on the number of atoms involved in the solvation. It is possible to extract radial-distribution functions from low energy Molecular Dynamics or a MC calculations, but we opt instead to analyze the K^+–He distances with increasing cluster size. In Figure 5, an example of such an analysis is given for $n = 70$.

The helium-cation interaction is reduced to 5 cm^{-1} at 7 Å, and it is 1 cm^{-1} at 9 Å, hence any predictions outside this range may not be very accurate. However, the formation of the second and even the third shell is very clearly recognizable at this figure. A comparison of such plots for different sizes show that the second shell can accommodate around 23 helium atoms. The radius of this shell is around 5 Å. The third shell begins after this regime but here the interaction with the cation is very weak and our classical additivity scheme may no longer be valid. It is difficult to get a good estimate of the size of this shell. We have continued with the growth scheme up to $n = 100$ but their minima usually corresponds to the configurations that maximize He–He interactions.

We have also analyzed structures of KHe_n^+ from diffusion Monte Carlo calculations which will be published elsewhere [17]. In these calculations, the angular distributions between He atoms show very strongly localized character and a striking resemblance to those obtained from our optimizations. Hence, we believe that it is safe to use the classical approaches in the presence of charged impurities.

In summary, we have studied the solvation of K^+ in helium droplets and calculated the structural characteristics of the clusters formed in this process. The first two solvation shells are formed of 15 and 23 helium atoms. There is some resemblance to a third shell but an accurate determination of it is not possible due to the floppy nature of the potential at this regime.

EY thanks the Turkish Academy of Sciences, MY to ITU Research Fund for their support; FAG and EB acknowledge computational support from the CASPUR consortium and from the INTAS project.

References

1. J.P. Toennies, A.F. Vilesov, Angewandte Chemie **43**, 2622 (2004)
2. P. Claas, S.O. Mende, F. Stienkemeier, Rev. Sci. Instrum. **74**, 4071 (2003)
3. J.P. Toennies, A.F. Vilesov, Annu. Rev. Phys. Chem. **49**, 1 (1998)
4. D.E. Galli, M. Buzzacchi, L. Reatto, J. Chem. Phys. **115**, 10239 (2001)
5. D. Bellet, W.H. Breckenridge, Chem. Rev. **102**, 1595 (2002)
6. C. Di Paola, F. Sebastianelli, E. Bodo, I. Baccarelli, F.A. Gianturco, M. Yurtsever, J. Chemical Theory and Computation **1**, 1045 (2005)
7. F. Sebastianelli, I. Baccarelli, E. Bodo, C.D. Paola, F.A. Gianturco, M. Yurtsever, Comput. Mat. Sci. **35**, 261 (2006)
8. E.P.F. Lee, T.G. Wright, Chem. Phys. Lett. **363**, 139 (2002)
9. T. Leininger, A. Nicklass, W. Kchle, H. Stoll, M. Dolg, A. Bergner, Chem. Phys. Lett. **255**, 274 (1996)
10. H.J. Werner et al., `www.molpro.net`
11. L.A. Viehland, Chem. Phys. **85**, 291 (1984)
12. R. Moszynski, B. Jeziorski, G.H.F. Diercksen, L.A. Viehland, J. Chem. Phys. **101**, 4697 (1994)
13. K.T. Tang, J.P. Toennies, J. Chem. Phys. **118**, 4976 (2003)
14. J.P.K. Doye, D.J. Wales, J. Phys. Chem. A **101**, 5111 (1997)
15. F. Calvo, E. Yurtsever, Phys. Rev. B **70**, 045423 (2004)
16. The Cambridge Cluster Database, URL `http://www-wales.ch.cam.ac.uk`
17. E. Coccia, E. Bodo, F.A. Gianturco, E. Yurtsever, M. Yurtsever, E. Yildirim, J. Chem. Phys. (submitted)